

## Article

# Formulation and Characterization of Non-Toxic, Antimicrobial, and Alcohol-Free Hand Sanitizer Nanoemulgel Based on Lemon Peel Extract

Faten Mohamed Ibrahim <sup>1,\*</sup>, Eman Samy Shalaby <sup>2</sup>, Mohamed Azab El-Liethy <sup>3</sup>, Sherif Abd-Elmaksoud <sup>4</sup>, Reda Sayed Mohammed <sup>5</sup>, Said I. Shalaby <sup>6</sup>, Cristina V. Rodrigues <sup>7</sup>, Manuela Pintado <sup>7,\*</sup> and El Sayed El Habbasha <sup>8</sup>

- <sup>1</sup> Medicinal and Aromatic Plants Research Department, Pharmaceutical and Drug Industries Research Institute, National Research Centre, Cairo P.O. Box 12622, Egypt
- <sup>2</sup> Pharmaceutical Technology Department, Pharmaceutical and Drug Industries Research Institute, National Research Centre, Cairo P.O. Box 12622, Egypt; dremanshalaby\_nrc@hotmail.com
- <sup>3</sup> Environmental Microbiology Lab., Water Pollution Research Department, National Research Centre, Dokki, Giza 12622, Egypt; mohamedazabr@yahoo.com
- <sup>4</sup> Environmental Virology Lab., Water Pollution Research Department, National Research Centre, Dokki, Giza 12622, Egypt; sherifnrc@yahoo.com
- <sup>5</sup> Pharmacognosy Department, Pharmaceutical and Drug Industries Research Institute, National Research Centre, Cairo P.O. Box 12622, Egypt; redamohammed2015@gmail.com
- <sup>6</sup> Complementary Medicine Department, National Research Centre, Cairo P.O. Box 12622, Egypt; saidshalaby7@gmail.com
- <sup>7</sup> CBQF—Centro de Biotecnologia e Química Fina—Laboratório Associado, Escola Superior de Biotecnologia, Universidade Católica Portuguesa, Rua Diogo Botelho 1327, 4169-005 Porto, Portugal; civrodrigues@ucp.pt
- <sup>8</sup> Field Crops Research Department, National Research Centre, Cairo P.O. Box 12622, Egypt; sayedhabasha@yahoo.com
- \* Correspondence: fatenmibrahim@gmail.com (F.M.I.); mpintado@ucp.pt (M.P.)



**Citation:** Ibrahim, F.M.; Shalaby, E.S.; El-Liethy, M.A.; Abd-Elmaksoud, S.; Mohammed, R.S.; Shalaby, S.I.; Rodrigues, C.V.; Pintado, M.; Habbasha, E.S.E. Formulation and Characterization of Non-Toxic, Antimicrobial, and Alcohol-Free Hand Sanitizer Nanoemulgel Based on Lemon Peel Extract. *Cosmetics* **2024**, *11*, 59. <https://doi.org/10.3390/cosmetics11020059>

Academic Editor: Vasil Georgiev

Received: 27 February 2024

Revised: 29 March 2024

Accepted: 9 April 2024

Published: 12 April 2024



**Copyright:** © 2024 by the authors. Licensee MDPI, Basel, Switzerland. This article is an open access article distributed under the terms and conditions of the Creative Commons Attribution (CC BY) license (<https://creativecommons.org/licenses/by/4.0/>).

**Abstract:** Recently, hand sanitization has gained attention for preventing disease transmission. Many on-the-market convenient dermal sanitizers contain alcohol, which can be detrimental to the skin. Therefore, three nanoemulgel formulations (LN-F1, LN-F2, LN-F3) incorporating lemon peel extract (LE), and with various increasing concentrations of xanthan gum as a gelling agent and stabilizer, were developed and characterized as a novel alternative. All formulations showed non-Newtonian shear-thinning flow behavior, particle size values below 200 nm, and increasing zeta potential with higher xanthan gum concentrations. All nanoemulgel formulations exhibited greater in vitro phenolic compound release than free LE. LN-F2 (1.0% LE, 20.0% mineral oil, 20.0% Span 80, 4.0% Cremophor RH 40, 4.0% PEG 400, 0.5% xanthan gum, 50.5% dH<sub>2</sub>O) was selected as the optimal formulation due to improved characteristics. LE and LN-F2 potential cytotoxicity was assessed on MA-104, showing no significant cellular morphological alterations up to 10 mg/mL for both samples. LN-F2 showed in vitro antimicrobial activity against *E. coli*, *S. Typhimurium*, *P. aeruginosa*, *S. aureus*, *L. monocytogenes*, and *C. albicans*, as well as antiviral activity against phiX 174, but no effect against rotavirus (SA-11). *In vivo*, LN-F2 presented a removal capacity of 83% to 100% for bacteria and 89% to 100% for fungi. These findings suggest that the formulated nanoemulgel holds potential as a safe and effective antiseptic, providing a viable alternative to commercial alcohol-based formulations.

**Keywords:** lemon peels; plant-based antimicrobial agents; bioactive compounds; sustainable nanoemulgel formulations; dermal sanitizer

## 1. Introduction

Nowadays, hand sanitizing has become part of most people's daily routine, primarily aimed at neutralizing various pathogens that can be transmitted through contaminated surfaces [1]. This prophylactic measure not only helps safeguard the user from potential

infection by these pathogenic microorganisms but also contributes to preventing their transmission, thereby reducing the risk of infectious disease propagation [2]. Moreover, due to the global pandemic caused by SARS-CoV-2, this practice has been increasingly adopted worldwide, due to the continuous and on-the-go necessity for hand hygiene [3]. Therefore, dermal sanitizers that allow for direct application to the skin without the need for rinsing have been developed and optimized, aiming to enhance the convenience of hand disinfection. A hand sanitizer is typically characterized as a liquid gel or foam developed to eliminate viruses, germs, and various other microorganisms from the hands [3]. Moreover, it can be categorized into two main types: alcohol-based (ABHS) and alcohol-free hand sanitizer. Dermal alcohol-based products have been commonly used for their safety and effective antisepsis properties, attributed to their antimicrobial capacities [2]. However, the use of ABHS may have some drawbacks, such as causing skin dryness [2], which can compromise the skin's barrier with prolonged use. On the other hand, alcohol-free hand sanitizers are generally considered safer, as they are less abrasive to the skin's barrier [3].

*Citrus limon* belongs to the *Rutaceae* family and is one of the most important fruit crops, growing widely in tropical and subtropical regions. According to the Food and Agriculture Organization (FAO), the global production of citrus exceeded 140 million tons in 2019 [4]. Besides being consumed as fresh produce, citrus fruits undergo processing into juice, canned or dehydrated products, marmalades, jams, and flavoring agents. Moreover, approximately 50–60% of the fruit weight, including peels, seeds, and pulps, is discarded after processing. These by-products contain several compounds such as vitamins, minerals, phenolic compounds, terpenoids, and dietary fiber which have different bioactivities [5,6]. For instance, *C. limon* has been extensively cultivated for its alkaloids present in crude extracts obtained from different parts of the fruit, which have demonstrated antibacterial potential against clinically relevant bacterial strains (e.g., *Escherichia coli*, *Staphylococcus aureus*, and *Salmonella* spp.) [7]. Additionally, these fruits are also important sources of other compounds of interest, such as polyphenols, which are bioactive molecules widely found in plant species, affecting their morphology, growth, reproduction, and resistance to pathogens and environmental stresses. Flavonoids, the most common group of polyphenols in plants, play crucial roles in plant responses and exhibit a broad spectrum of biological activity such as antibacterial, antifungal, antidiabetic, anticancer, and antiviral properties [7,8]. The most abundant flavonoids identified in citrus are naringin, hesperidin, narirutin, and neo-hesperidin [9].

Traditional topical vehicles, including lotions, ointments, patches, and creams, are associated with disadvantages such as poor penetrability. Furthermore, they may exhibit undesirable physicochemical characteristics, with a lower spreading coefficient, requiring rubbing and resulting in a more difficult application. In addition, ensuring the stability of these formulations can also be an issue. However, it has been reported that topical nanosized formulations can offer a viable solution to these concerns by promoting drug delivery through the induction of temporary disruption in the highly organized lipid bilayer structure of the skin. These formulations are also advantageous due to their low irritation to the skin, high stability, and improved local activity [10,11]. For instance, nanoemulsions are characterized as transparent and thermodynamically stable systems with droplet sizes of 20–200 nm, composed of oils and surfactants usually in association with co-surfactants. Despite their many benefits, low viscosity and spreadability are the main disadvantages of topical nanoemulsion formulations. Based on this knowledge, attempts have been made to formulate nanoemulgels by combining nanoemulsions with gelling agents, aiming to achieve a formulation with non-staining, thixotropy, emollient, non-greasy properties and improved spreadability [12]. Moreover, for individuals sensitive to alcohol-based formulations, incorporating a less abrasive substance, such as lemon peel extract with antimicrobial activities, into a nanoemulgel formulation could present a promising opportunity for hand hygiene. Therefore, the objective of the present study is to develop and characterize a non-toxic and alcohol-free nanoemulgel based on an upcycled lemon peel extract for hand-sanitizing purposes. Moreover, this research aims to

address literature gaps regarding sustainable and effective hand sanitization ingredients, which is essential for advances in the field of resistant-pathogen-targeting formulations, representing a viable alternative to commercial alcohol-based solutions.

## 2. Materials and Methods

### 2.1. Chemicals

The sorbitan monooleate (Span 80) was acquired from LobaChemie (Mumbai, Maharashtra, India). Xanthan gum (Rheocare® XGN) and polyethylene glycol hydrogenated castor oil (CREMOPHOR® RH 40), were obtained from BASF (Ludwigshafen am Rhein, Germany). Polyethylene glycol 400 (PEG 400) was obtained from Sigma-Aldrich (St. Louis, MO, USA). Liquid paraffin, potassium monohydrogen phosphate, and dipotassium hydrogen phosphate were purchased from El Nasr Pharmaceutical Chemicals (Cairo, Egypt). Trypticase soy broth and Mueller–Hinton agar were obtained from BBL (Darmstadt, Germany). Malt extract agar was obtained from Merck (Merck, St. Louis, MO, USA, Sigma-Aldrich, St. Louis, MO, USA). The standard plate count agar was obtained from Hach (Ames, IA, USA). All reagents were used as received.

### 2.2. Raw Materials and Sample Preparation

The lemons (*Citrus limon*) used to obtain the bioactive extract were freshly collected at the National Research Center Farm (Agricultural Production and Research Station, National Research Center, El Nubaria Province, El Behira Governorate). The lemon peels were then removed from the fruit and used as needed.

### 2.3. Microbial Strains' Growth Conditions

*Escherichia coli* (ATCC 25922), *Salmonella enterica* serovar Typhimurium (ATCC 14028), *Pseudomonas aeruginosa* (ATCC 10145), *Staphylococcus aureus* (ATCC 43300), *Listeria monocytogenes* (ATCC 35152), and *Candida albicans* (ATCC 10231) were cultured in Mueller–Hinton medium (BBL, Darmstadt, Germany). These microbial cultures were prepared by inoculating the medium with each test microbe and incubating at 35 °C for 24 h. Microbial cells were obtained by centrifuging each culture under sterile conditions at 4000 rpm for 15 min. The cells were washed with 20 mL of sterile phosphate-buffered saline (PBS) and centrifuged (4000 rpm for 5 min) until the supernatant became clear. The optical density for each suspension was recorded at 500 nm, and serial dilutions were carried out using appropriate aseptic techniques until the optical density was between 0.5 and 1.0. The number of colony-forming units was assessed to guarantee a concentration of  $5.0 \times 10^6$  CFU/mL.

### 2.4. Cell Culture Growth Conditions

The MA-104 cell line (Holding Company for Biological Products & Vaccines VAC-SERA, Agouza, Giza, Egypt) was cultured in Dulbecco's modified Eagle's medium—high glucose (DMEM, Gibco™). The cell culture was incubated at 37 °C in a humidified incubator containing 5% CO<sub>2</sub>, and the medium was replaced every 2 to 3 days until an 85% confluence of cells was achieved. After cell trypsinization using TrypLE Express (Gibco™), the cells were counted in a hemocytometer and seeded into 96-well plates (Greiner-Bio one, Frickenhausen, Germany) at a density of  $5.0 \times 10^4$  cells/mL. The cells were then left to adhere for 24 h.

### 2.5. Lemon Peel Extraction Methodology

To develop the nanoemulgel formulation, a hydroethanolic extraction process was conducted to acquire a polyphenolic-rich extract from the peels of *Citrus limon* (LE). Briefly, the fresh peels were weighed and macerated for 24 h using 80% (v/v) ethanol in a 1:3 (w/v) ratio. The resulting mixture was then filtered and concentrated through vacuum-drying using a rotary evaporator at 45 °C. The obtained extract was stored at 4 °C in an amber bottle until further use.

## 2.6. Antimicrobial Activity of the Lemon Peel Extract (LE)

The antimicrobial activity of LE was assessed through minimum inhibitory concentration (MIC) and minimum microbicidal concentration (MMC) determination against *Staphylococcus aureus* (ATCC 6538, Gram-positive), *Escherichia coli* (ATCC 25922, Gram-negative), and *Candida albicans* (ATCC 10231, yeast). LE was diluted in dimethyl sulfoxide (DMSO) to obtain a stock solution of 5 mg/mL, followed by two-fold dilutions to achieve several testing concentrations. To a 96-well plate, 100 µL of each microbial suspension ( $5.0 \times 10^6$  CFU/mL) and 100 µL of each LE dilution were added per well. As a positive control of microbial growth, medium with only DMSO (without LE) was used. The inoculated microplates were loosely wrapped with Parafilm and incubated at 37 °C for 18–24 h.

The resazurin solution was prepared by dissolving 67.5 mg of resazurin dye in 10 mL of dH<sub>2</sub>O, followed by vortex homogenization. The solution was sterilized by filtration using a membrane filter with a pore size of 0.22–0.45 µm. Afterward, 10 µL of this dye solution was added to each testing and control well, and an additional 4 h of incubation was carried out. The color changes within each well upon resazurin incubation were analyzed. The MIC value was defined as the lowest concentration of LE at which color change was observed.

Using an inoculation loop, samples were taken from each well corresponding to the two lowest concentrations right before the MIC value for each strain and spread on sterile nutrient agar plates. The plates were incubated at 35 °C for 24 h. MMC was taken as the lowest sample concentration that did not exhibit any microbial growth. Each test condition was performed in duplicate.

## 2.7. Preparation of Lemon-Extract-Based Nanoemulgel (LN) Formulations

The nanoemulgels loaded with lemon peel extract (LN) were prepared in two phases: phase A and phase B. Phase A was prepared by mixing LE, surfactants (Span 80 and Cremophor RH 40), and oils (PEG 400 and mineral oil) to obtain the nanoemulsion. This mixture was stirred at 1500 rpm using a mechanical stirrer and vortexed (2000 rpm, 5 min). For phase B, dH<sub>2</sub>O was slowly added to xanthan gum and mechanically stirred until a homogenous polymeric soluble gel was formed. The extract-loaded emulsion (phase A) was then slowly added to the polymeric gel base (phase B) and then mixed under magnetic stirring for 5 min until a homogenous gel was obtained [13]. The final lemon peel extract content was 10 mg/g of nanoemulgel for all tested formulations. This extract concentration was chosen for its improved antimicrobial capacity. The composition of each LN formulation (LN-F1, LN-F2, and LN-F3) is detailed in Table 1.

**Table 1.** Composition of the developed nanoemulgel formulations (LN-F1, LN-F2, and LN-F3), based on *Citrus limon* peel extract (LE).

Ingredients (g)		Formulations		
		LN-F1	LN-F2	LN-F3
Phase A	LE	0.100	0.100	0.100
	Mineral Oil	2.000	2.000	2.000
	Span 80	2.000	2.000	2.000
	Cremophor RH 40	0.400	0.400	0.400
	PEG 400	0.400	0.400	0.400
Phase B	Xanthan Gum	0.025	0.050	0.100
	Water (dH <sub>2</sub> O)	5.075	5.050	5.000

## 2.8. Fourier Transform Infrared (FTIR) Spectroscopy Characterization of LE and LN Formulations

The chemical integrity and potential chemical interactions between LE and the components of LN formulations were assessed using FTIR spectrophotometry (JASCO 6100, Tokyo, Japan). Xanthan gum was mixed separately with potassium bromide and compressed (200 kg/cm<sup>2</sup>, for 2 min) in a hydraulic press to form a compact disk. In contrast,

the liquid samples (LE, LN formulations, and the remaining individual ingredients) were analyzed directly. All samples were scanned against a blank KBr pellet background in the spectral region between  $4000\text{ cm}^{-1}$  and  $400\text{ cm}^{-1}$  [14,15]. The resolution used was  $4\text{ cm}^{-1}$ , and each spectrum was acquired by an average of 32 scans, in transmission mode.

### 2.9. Organoleptic Properties and Phase Separation Evaluation of LN Formulations

Firstly, the LN formulations' organoleptic properties, namely texture and color, were macroscopically evaluated. Also, to evaluate the occurrence of phase separation under extreme conditions, all LN formulations were subjected to centrifugation. Accordingly, 5 g of each nanoemulgel formulation was centrifuged at 5000 rpm for 30 min at room temperature [16–18]. Subsequently, the samples were examined regarding phase separation. Triplicates were made for this assessment.

### 2.10. Rheology Analysis of LN Formulations

Rheological measurements of the developed LN formulations were acquired using a parallel-plate rheometer (Physica MCR 301, Anton Paar GmbH, Graz, Austria). Measurements were conducted to determine shear viscosity as a function of shear rate. A total of 25 measurement points were acquired with shear rates ranging from  $1\text{ s}^{-1}$  to  $250\text{ s}^{-1}$  [19], at  $25.0 \pm 0.1^\circ\text{C}$ . The plot was obtained from the average of duplicates.

### 2.11. Particle Size, Polydispersity Index, Zeta Potential, and pH Analysis of LN Formulations

The physical characteristics of the LN nanoemulsions, including particle size (PS), polydispersity index (PDI), and zeta potential (ZP), were assessed at  $25.0 \pm 2.0^\circ\text{C}$  by diluting each formulation at a ratio of 1:100 (*v/v*) in dH<sub>2</sub>O [19]. These analyses were conducted using photon correlation spectroscopy with a Malvern Zetasizer (ZS, Malvern Instruments, Ltd., Worcestershire, UK). Additionally, the pH of the LN formulations was assessed under the same temperature conditions using a pH meter Orion Versa Star™, Thermo Fisher Scientific, Waltham, MA, USA).

### 2.12. In Vitro Polyphenolic Content Release of LE and LN Formulations

The in vitro polyphenolic content release profile from LE and LN formulations was analyzed by dialysis [20]. An amount equivalent to 15 mg of extract for both LE and LN formulation testing was placed into the dialysis membrane (cellulose membrane, molecular weight cut-off of 12,000–14,000, Sigma-Aldrich Co., St. Louis, MO, USA). This procedure was conducted against 100 mL of acetate buffer (pH 5.5) [20] and a 10% ethanol (*v/v*) solution [21], in a shaking water bath (MemmertSV-1422, Memmert GmbH, Schwabach, Germany) at  $32.0 \pm 0.5^\circ\text{C}$ , 100 rpm. Samples were withdrawn every 2 h, up until the 24 h time point, to measure the polyphenol concentration spectrophotometrically, using the UV-2401 PC (Shimadzu Co., Kyoto, Japan). The release profile of the phenolic compounds from the selected formulations was compared to the raw lemon extract polyphenol solution containing the same extract concentrations. The cumulative percentage of phenolic compounds released was determined as the ratio between the quantity of total polyphenols released ( $C_f$ ) and the initial quantity of total phenolic compounds inserted in the dialysis membrane ( $C_i$ ) (Equation (1)). All measurements were carried out in triplicate. Different release mathematical models were employed to elucidate the release mechanism. This analysis included the zero order, first order, Higuchi model, and Korsmeyer–Peppas models [22].

$$\text{Polyphenols Release Quantity (\%)} = C_f/C_i \times 100 \quad (1)$$

### 2.13. Identification and Quantification of LN-F2 Phenolic Content by LC-ESI-MS/MS

The phenolic content analysis of LN-F2 was performed by liquid chromatography–electrospray ionization–tandem mass spectrometry (LC-ESI-MS/MS) with an Exion LC AC system for separation and SCIEX Triple Quad 5500+ MS/MS system equipped with electrospray ionization (ESI) for detection. The separation was performed using a ZORBAX

Eclipse Plus C18 Column (4.6 × 100 mm, 1.8 µm). The mobile phases consisted of two eluents: (A) 0.1% (*v/v*) aqueous formic acid and (B) LC-grade acetonitrile. The mobile phase was programmed as follows: 0–1 min, 2% B; 1–21 min, 2–60% B; 21–25 min, 60% B; 25.01–28 min, 2% B at a flow rate of 0.8 mL/min and an injection volume of 3 µL. For MRM analysis of the selected phenolic compounds, negative ionization modes were applied: curtain gas, 25 psi; ion spray voltage, 4500 V; temperature source, 400 °C; ion gas source 1 and 2, 55 psi; declustering potential, 50 V; collision energy, 25 V; collision energy spread, 10%. This analysis was conducted in triplicate.

#### 2.14. LN-F2 Transmission Electron Microscopy (TEM) Characterization

The selected nanoemulgel system (LN-F2) was characterized through transmission electron microscopy (TEM) (JEM-2100, JEOL Co., Tokyo, Japan) to evaluate its components' morphological attributes, including lamellarity, shape, and size.

#### 2.15. LE and LN-F2 Cytotoxicity Evaluation by Inverted Light Microscopy Analysis

This test was conducted to evaluate the potential cytotoxic concentrations of LE and LN-F2 [23]. Concentrations ranging from 10 µg/100 µL to 1 mg/100 µL for each sample were prepared using Dulbecco's Modified Eagle's Media (DMEM). Additionally, MA-104 cells (2 × 10<sup>5</sup> cells/mL) were prepared in 96-well culture plates (Greiner-Bio one, Germany). After confluence, the medium was removed from the wells and replaced with 100 µL of each prepared testing concentration. As a negative control of cytotoxicity, 100 µL of DMEM without any sample was used. The cells were incubated at 37 °C in a humidified atmosphere containing 5% CO<sub>2</sub> for 72 h. Cell morphology was microscopically analyzed at 24, 42, and 72 h after sample incubation to evaluate any potential morphological alterations, such as loss of confluence, cell rounding and shrinking, cytoplasm granulation, and/or vacuolization [23].

#### 2.16. LE and LN-F2 Bioactivity Assessment

##### 2.16.1. In Vitro Antiviral Activity

The antiviral activity of LE and LN-F2 was analyzed against rotavirus SA-11 and the bacteriophage phiX 174. For this purpose, LE was prepared at 10 mg/mL, while LN-F2 was prepared at 1 and 10 mg/mL, using sterile dH<sub>2</sub>O with 10% (*v/v*) dimethyl sulfoxide (DMSO).

##### Viruses' Propagation Conditions

Rotavirus was activated with 10 µg/mL trypsin before propagation on MA-104 cells. Centrifugation of the rotavirus was performed at 1000× g for 5 min in order to purify the sample by removing cell debris. After filtration through a 0.2 µm membrane, the supernatant was kept and used as a virus stock suspension, containing 10<sup>6</sup>–10<sup>7</sup> TCID<sub>50</sub>/mL. The suspension was then stored at –80 °C until further use.

Bacteriophage phiX 174 was propagated in an *E. coli* DSM 13127 host, in 3.0% trypticase soy broth (TSA) (BD, Franklin Lakes, NJ, USA) containing 0.1% glucose, 2 mM CaCl<sub>2</sub>, and 10 mg/mL thiamine, at 37 °C for 18 h. The bacteriophage was then harvested by centrifugation and filtration using the abovementioned procedure for rotavirus.

##### Viruses' Quantification

Virus quantification was performed on cells exposed to each virus, either untreated or after treatment with LE or LN-F2. Moreover, the 50% tissue culture infectious dose (TCID<sub>50</sub>), a parameter used to quantify and assess the infectivity of a virus in cells, defined as the virus solution concentration at which 50% of the cells show cytopathic effects (CPE), was also assessed during this assay.

The infectivity of the rotavirus SA-11 stock was activated by adding 10 µg/mL trypsin for 30 min at 37 °C. A 100 µL aliquot of the activated rotavirus SA-11 at a final concentration of 1.0 × 10<sup>6</sup> TCID<sub>50</sub>/mL was mixed with an equal volume of LE (10 mg/mL) or LN-F2

(containing 1 mg/mL or 10 mg/mL of LE) at the prepared concentrations. The different solutions containing rotavirus with each sample underwent an initial incubation at 37 °C, for 30 min, followed by mixing and subsequent incubation for an additional 60 min.

After MA-104 cells adhered onto 96-well plates, the cells were incubated with the activated rotavirus suspension, as a positive control of cytotoxicity, or with the various sample (10 mg/mL of LE, 1 mg/mL of LN-F2, or 10 mg/mL of LN-F2) solutions containing rotavirus, for 7 days, at 37 °C, under a humid atmosphere containing 5% CO<sub>2</sub>. During the seven days of incubation, cells were microscopically monitored daily to check for CPE, and the TCID<sub>50</sub> was analyzed. This analysis was performed in duplicate for each sample.

To assess the effect of the testing solutions on the phiX 174 bacteriophage, equal volumes of virus suspension and each sample were mixed and incubated for 30 min, at 37 °C, as described previously. The viral titer after each treatment was evaluated by standard plaque assay. Briefly, 0.9 mL of phage sample solution and 0.1 mL of *E. coli* culture solution were added to 0.6% molten top agar (BD, Franklin Lakes, NJ, USA), mixed, and poured on tryptic soy agar (TSA) (BD, Franklin Lakes, NJ, USA) plates. The plates were incubated at 37 °C overnight, and then the colony-forming units were counted. The virus inhibition after treatment with each sample was calculated as the difference between initial ( $V_i$ ) and final ( $V_f$ ) virus counts, according to Equation (2). This assessment was carried out in duplicate.

$$\text{Virus inhibition (\%)} = (V_i - V_f)/V_i \times 100 \quad (2)$$

#### 2.16.2. In Vitro and In Vivo LN-F2 Antimicrobial Activity

##### Zone of Inhibition (ZI) Analysis by Well and Disk Diffusion Assays

LN-F2 antimicrobial properties were assessed in vitro through the disk and well diffusion techniques, against Gram-positive bacterial strains: *Staphylococcus aureus* (ATCC 43300), *Listeria monocytogenes* (ATCC 35152); Gram-negative bacterial strains: *Escherichia coli* (ATCC 25922), *Salmonella enterica* serovar Typhimurium (ATCC 14028), *Pseudomonas aeruginosa* (ATCC 10145); and a yeast: *Candida albicans* (ATCC 10231). Each microbial strain was added to a tube containing trypticase soy broth (BBL, Germany). The inoculation tubes were kept at 37 °C for 24–48 h.

To carry out both tests, the inoculated microorganisms were cultivated in Mueller–Hinton agar plates, using sterile cotton swabs. For the disk diffusion method, sterile disks (6 mm in diameter) were submerged in the developed LN and then were aseptically transferred to the center of each cultured agar plate surface. For the well diffusion test, wells were excavated in the cultured Mueller–Hinton agar media plates, using sterile tips. Following that, 100 μL of the testing LN was added to the wells. Regarding both tests, all plates were then incubated for 24–48 h at 37 °C. After incubation, the zone of inhibition (ZI) was measured in mm, using a measuring ruler (HiMedia Co., Maharashtra, India).

##### In Vivo Assessment

The in vivo testing of the LN-F2 antimicrobial properties was carried out according to the protocols outlined by Public Health England [24] and Lambrechts et al. [25]. Briefly, samples were collected from 20 healthy volunteers, with ages ranging from 25 to 67 years and of different genders, both before and after the application of LN-F2 (2.0 g). A 5.0 × 5.0 cm<sup>2</sup> area of volunteers' hands was scrubbed using sterile swabs, which were then placed in a tube filled with 5 mL of sterile dH<sub>2</sub>O. The same procedure was repeated after applying 2.0 mg of LN-F2 on the volunteers' hands, and the nanoemulgel was fully absorbed by the skin. The tubes were then vortexed for 30 s.

In accordance with the American Public Health Association's (APHA) recommended procedure [26], total bacterial and total fungal counts were determined for all collected samples. The total fungal counts were conducted using the pour plate method on malt extract agar (MEA), while total bacterial counts were determined through standard plate count (SPC) agar. For bacteria, the inoculation plates were incubated at 37 °C for 24–48 h, while fungi were incubated for 48–72 h. Microbial counts were estimated using the colony

counter model SC6PLUS (Stuart, UK). The viable microbial cell density was calculated and expressed by CFU/cm<sup>2</sup>. The removal efficiency (R%) of the total bacterial and fungal counts was calculated according to Equation (3).

$$R (\%) = (ib - ia)/ib \times 100 \quad (3)$$

where ib represents microbial counts before the addition of the LN-F2, and ia represents microbial counts after the addition of the LN-F2.

### 2.17. Statistical Analysis

Experiments were conducted in duplicate or triplicate, and values were expressed as mean  $\pm$  standard deviation (SD). IBM® SPSS® Statistics (version 25) was used to perform the statistical analysis, using the one-way ANOVA and post hoc tests for multiple comparisons. Statistical significance was established at  $p$ -value  $< 0.05$ . Data processing and plot development were carried out using Microsoft Excel 2016.

## 3. Results and Discussion

### 3.1. Lemon Peel Extract Antimicrobial Activity

After obtaining the lemon peel extract (LE), the potential in vitro antimicrobial activity was assessed through MIC and MMC determination.

The MIC value, representing the minimum concentration at which a compound inhibits the growth of a specific microorganism, is a standard measure of antimicrobial efficacy [27,28]. The MMC value, indicating the lowest concentration required to eliminate 99.9% of a microorganism, is also crucial in assessing antimicrobial effectiveness [29]. Therefore, to gain further insights into the potential antimicrobial capacity of the obtained LE, its MIC and MMC values were assessed against *E. coli* (Gram-negative), *S. aureus* (Gram-positive), and *C. albicans* (yeast). As shown by the results presented in Figure 1, the extract demonstrated low MIC values against all tested microorganisms, namely  $156.25 \pm 3.50 \mu\text{g}/\text{mL}$  for *S. aureus*,  $78.13 \pm 2.85 \mu\text{g}/\text{mL}$  for *E. coli*, and  $19.53 \pm 1.08 \mu\text{g}/\text{mL}$  for *C. albicans*. Regarding the MMC results, LE also presented relatively low values against *E. coli* ( $78.13 \pm 1.91 \mu\text{g}/\text{mL}$ ) and *C. albicans* ( $78.13 \pm 1.57 \mu\text{g}/\text{mL}$ ), while for *S. aureus*, those values were notably higher ( $625.00 \pm 5.60 \mu\text{g}/\text{mL}$ ). Nonetheless, for each microorganism, the MIC and MMC values were correlated and followed the same tendency.

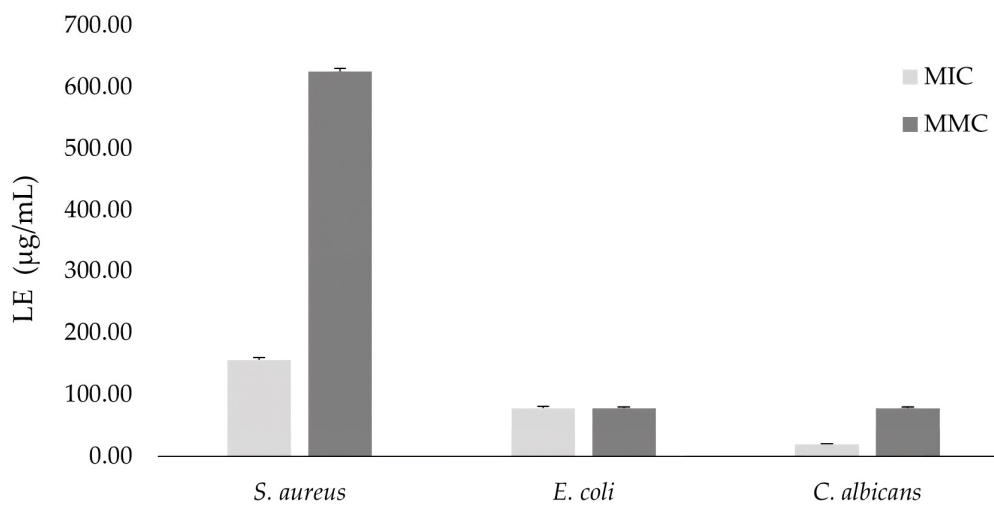


**Figure 1.** Minimum inhibition concentration (MIC) and minimum microbicidal concentration (MMC) of the lemon peel extract (LE) against *S. aureus*, *E. coli*, and *C. albicans*.

These findings align with existing literature, which also supports the antimicrobial efficacy of lemon peel extracts against several Gram-positive and Gram-negative bacteria, as well as *Candida* strains [30]. Henderson et al. [31] highlighted the antibacterial properties of

a lemon peel extract against *Escherichia coli*, *Staphylococcus aureus*, *Salmonella enteritidis*, and *Listeria monocytogenes*. Jonh et al. [32] also reported that employing different solvents during the extraction process might result in extracts with varying antimicrobial capacity, showing the impact of the extraction method on the antimicrobial effectiveness of the extract. For instance, the authors demonstrated that the methanolic extract showed higher activity against *S. flexneri*, *S. aureus*, and *E. coli*, while the acetone extract was only effective against *S. aureus* and *E. coli*, and the ethanolic extract presented higher antimicrobial capacity against *P. aeruginosa* and *S. enterica* serovar Typhimurium.

According to Saleem et al. [33], the LE antimicrobial effect might be mainly related to the presence of bioactive compounds such as phenolic compounds in the lemon peel. Overall, the extract exhibited a higher antimicrobial effect on *E. coli* and *C. albicans*, attributed to the ability of the bioactive compounds present in LE to attach to the outer membrane of Gram-negative bacteria, compromising its integrity and leading to the release of cytoplasmatic content and cell death [34]. Furthermore, Henderson et al. [31] explained that LE can have antimicrobial properties through the degradation of lipids and proteins constituting the microorganism's membranes, resulting in their disruption. Nonetheless, it has also been stated that the thicker peptidoglycan layer in the cell walls of Gram-positive bacteria can be infiltrated by some bioactive compounds found in lemon peels [35,36], which can explain LE's effectiveness against *S. aureus*.

### 3.2. Development of LE-Based Nanoemulgel Formulations

After assessing the antimicrobial activity of the LE, three different formulations (LN-F1, LN-F2, and LN-F3) were developed and subsequently characterized, aiming to achieve an optimal LE-based nanoemulgel (LN) (Figure 2) for potential hand-sanitizing applications. An LE extract concentration of 10 mg/g was chosen to develop all LN formulations to guarantee an effective antimicrobial activity. Regarding the chosen gelling agent, a variety of compounds, such as Carbopol, poloxamer, tragacanth, and HPMC have been applied in the production of nanoemulgels. Nonetheless, xanthan gum was selected for the development of these LN formulations, due to its many physical–chemical and mechanical advantages. Xanthan gum offers higher viscosity even at low concentrations, unlike other polysaccharides, and its elastic properties make it an ideal stabilizer. Also, xanthan gum is highly resistant to pH variations, meaning that it is stable in both alkaline and acidic conditions. Moreover, xanthan gum has an improved thermal stability compared to other water-soluble hydrocolloids, providing a better stability to the formulation at a wide temperature range [37]. Despite xanthan gum being reported in the preparation of nanoemulgels, at concentrations up to 3% [10], it was concluded in previous studies that its incorporation up to 1% would produce the most suitable gel consistency, while maintaining its stability [38]. Therefore, a xanthan gum concentration between 0.25 and 1% was selected.

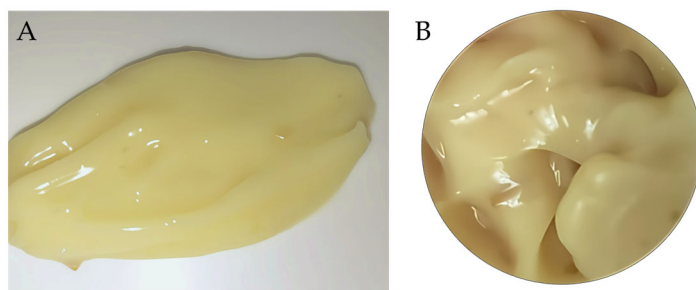


**Figure 2.** Macroscopic morphological profile of LN-F2, as an example of a lemon-peel-extract-based nanoemulgel formulation. (A) LN-F2 swatch, demonstrating the spreadability of the formulation; (B) LN-F2 inside a container, demonstration the formulation homogeneity.

In an initial macroscopic evaluation, all formulations demonstrated satisfactory spreadability (Figure 2A), homogeneity, and no indications of phase separation (Figure 2B), suggesting preliminary stability in the formulation [39]. Furthermore, there were no

notable distinctions observed among the three tested nanoemulgels, each formulated with varying concentrations (0.25 to 1.00%) of xanthan gum, used as a gelling agent and stabilizer, to create the polymeric base gel. Consequently, based on a first analysis, all formulations appeared to possess physical and morphological characteristics suitable for the intended application.

### 3.3. LE and LN Formulations' Physicochemical Analysis

#### 3.3.1. LE and LN Formulations' FTIR Analysis

The FTIR spectra of LE and LN formulations, as well as of the individual formulation components (Figure 3), were acquired to characterize their chemical structure and the interaction between compounds within formulations.

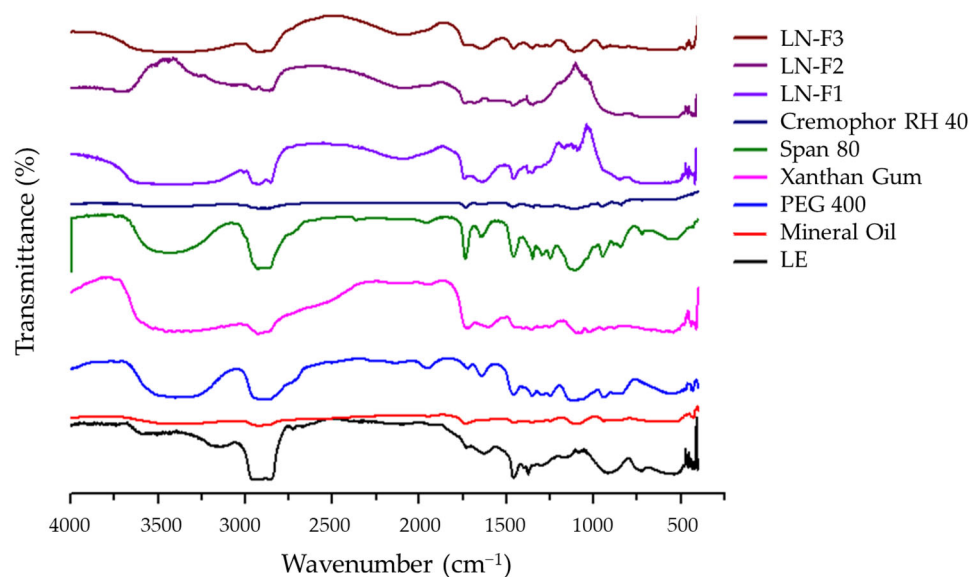


**Figure 3.** FTIR spectra of the individual components of the tested formulations (mineral oil, PEG 400, xanthan gum, Span 80, and Cremophor RH 40), the lemon peel extract (LE), and the corresponding nanoemulgels (LN-F1, LN-F2, and LN-F3).

Regarding LE, the results indicated that its main component is naringinin, as evidenced by the reported peaks at 3285.79, 3117.36, 3035.80, 1629.76, 1602.09, 1519.88, 1498.10, and 1463.39  $\text{cm}^{-1}$  [40]. Moreover, when comparing the spectra of the nanoemulgels (LN-F1, LN-F2, and LN-F3) with LE, changes in peak intensity and position of various components were observed, corroborating the assembly of the nanoemulgel through different chemical interactions [41]. In detail, the individual analyzed components were LE, Span 80, Cremophor RH 40, mineral oil, and PEG 400. The characteristic peaks of these components resemble those described in the literature, suggesting highly purified samples suitable for nanoemulgel formulations [42]. Analyzing the LE spectrum, the peak at 2750  $\text{cm}^{-1}$  related to the -OH group of naringinin is shifted or fused in the IR spectra of the nanoemulgels, indicating an interaction between the ingredients and the extract and suggesting successful extract incorporation into the nanoemulgels [43]. On the other hand, the FTIR spectra of LN-F1, LN-F2, and LN-F3 showed the characteristic peaks of Span 80, PEG 400, and xanthan gum. However, most of the peaks were diffused, especially those related to the hydroxyl group, asymmetric and symmetric aliphatic C-H stretching, and C=O ester bond. The intensity of the peak for alkyl substituted ether in the Span 80 spectrum decreased upon incorporation into the nanoemulgel formulations. Additionally, the stretching vibration of the ester functional group (C-O-C) was observed between 1172 and 1102  $\text{cm}^{-1}$ . Furthermore, the intensity of LE characteristic peaks also decreased and shifted to a lower frequency after its formulation into the nanoemulgel (2915 and 2752  $\text{cm}^{-1}$  for the asymmetric and symmetric stretching vibrations of -CH<sub>2</sub>, 1450.3  $\text{cm}^{-1}$  for C=C stretching vibration,

and  $722\text{ cm}^{-1}$  for the C-H bend), with a minor shift noticed in the peak for C=C stretching vibration ( $1467.9\text{ cm}^{-1}$ ).

It is important to note that the LE peaks within the nanoemulgel formulations did not significantly shift, and no new peaks were observed. Overall, these findings indicate that the ingredients used to formulate the nanoemulgel did not significantly affect the chemical structure of LE, suggesting that the extract and its potential bioactivities were preserved after inclusion in the nanoemulgels [44].

### 3.3.2. LN Formulations' Organoleptic Properties, Phase Separation, and Rheology Analysis

In order to assess whether the LN formulations possessed adequate organoleptic and physical–chemical characteristics for hand sanitization applications, their color, texture, stability in terms of phase separation under extreme conditions, and rheological behavior were analyzed.

In terms of color and texture, all samples presented a light-yellow color, were homogenous, demonstrated reasonable consistency, and no signs of primary phase separation were observed. However, all formulations underwent centrifugation stress to test for the occurrence of creaming, cracking, or coalescence to analyze their stability under extreme conditions. The results indicated that only LN-F2 maintained its morphology after centrifugation, showing no visible signs of phase separation. However, LN-F1 and LN-F3 exhibited phase separation after being submitted to this assessment. These results might be attributed to the quantities of xanthan gum and dH<sub>2</sub>O used to formulate the polymeric gel base (phase B), specifically 0.025 g of xanthan gum and 5.075 g of dH<sub>2</sub>O for LN-F1, and 0.100 g of xanthan gum and 5.000 g of dH<sub>2</sub>O for LN-F3, leading to unstable o/w chemical interactions between the emulsion components and eventually resulting in phase separation [45].

Furthermore, for an ideal topical application, the formulation must be easily spreadable and non-dripping in nature. Regarding these results (Figure 4), all LN samples exhibited a Newtonian shear-thinning flow behavior, indicating a decrease in viscosity with increasing shear rate. Moreover, it was observed that the nanoemulgels' viscosity increased with higher xanthan gum concentrations. However, when the formulation is subjected to a shear force, its network structure breaks down, leading to a gradual decrease in viscosity. This shear-thinning property might be suitable for the target application, as it allows easier removal of the nanoemulgel from the container and facilitates its application on skin [46].

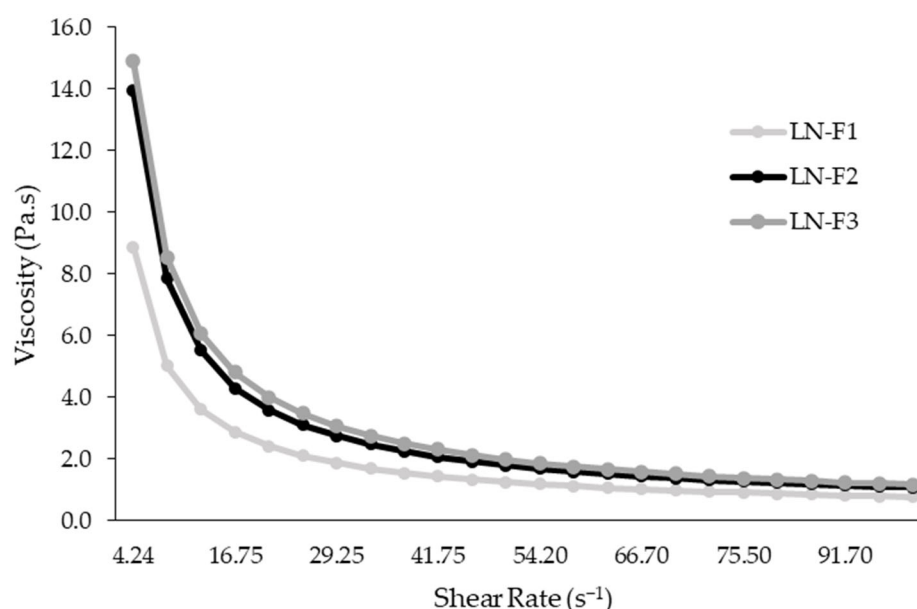


**Figure 4.** Rheogram of the three developed nanoemulgel formulations (LN-F1, LN-F2, and LN-F3). The plot is presented as an average of duplicates.

### 3.3.3. LN Formulations' Particle Size, Polydispersity Index, Zeta Potential, and pH Assessment

All LN formulations were characterized in terms of particle size (PS), polydispersity index (PDI), zeta potential, and pH (Table 2).

**Table 2.** Particle size, zeta potential, polydispersity index (PDI), and pH values of the developed nanoemulgel formulations (LN-F1, LN-F2, and LN-F3).

Formulation	Particle Size $\pm$ SD (nm)	Zeta Potential $\pm$ SD (mV)	PDI $\pm$ SD	pH $\pm$ SD
LN-F1	123.30 $\pm$ 0.18	-15.90 $\pm$ 1.97	0.422 $\pm$ 0.01	5.51 $\pm$ 0.24
LN-F2	152.80 $\pm$ 1.78	-43.60 $\pm$ 2.64	0.43 $\pm$ 0.06	5.59 $\pm$ 0.07
LN-F3	176.90 $\pm$ 4.36	-56.80 $\pm$ 3.77	0.46 $\pm$ 0.19	5.57 $\pm$ 0.73

As reported by Eid et al. [47], a slight increase in PS may occur due to the increment in viscosity, which is evident in the obtained results and aligns with the data obtained from the rheology assessment. Therefore, LN-F3, being the formulation with higher viscosity, also presented a higher PS value (176.90 nm). Moreover, the mean droplet size is below 200 nm in all formulations, consistent with previous results reported by Eid et al. [47]. The PDI is a valuable parameter to evaluate the stability of the nanoemulgel formulation, representing the distribution of a population's size within a given sample [48]. Since all LN formulations presented a PDI value lower than 0.5, it indicates a narrow and uniform particle size distribution within all samples [49]. On the other hand, the zeta potential is a relevant factor to assess the stability of nanosuspensions. According to the literature, acquiring a zeta potential of approximately  $\pm$  30 mV is typically ideal for the formulation of a stable solution. At this charge level, droplets exhibit repulsion, preventing coalescence and ensuring stability [50]. In this way, LN-F2 and LN-F3, showing a zeta potential greater than -30 mV, can be considered stable formulations, while LN-F1 presented a zeta potential value of -15.9 mV. Extremely positive or negative zeta potential values cause larger repulsive forces, whereas repulsion between particles with similar electric charges prevents aggregation of the particles, ensuring easy redispersion [51]. The negative surface charge of the nanoemulsion droplet might be explained by the mixture of Span 80 with Cremophor RH 40 ions, forming hydrogen bonds between the mixed surfactants and water molecules in the boundary layer of the o/w emulsion, in accordance with already reported results [52]. Regarding pH values, they were similar for all formulations (5.51–5.59).

### 3.4. In Vitro Release of the LE and LN Formulations' Polyphenolic Content

*Citrus limon* peel is highly rich in phenolic compounds, which have been studied for their antioxidant and antimicrobial capacities [8,53]. Therefore, the release profile of phenolic content from LE and LN formulations was analyzed. As shown in Figure 5, all the LN formulations released higher amounts of phenolic compounds than LE, emphasizing the benefits of using this carrier for delivering bioactive compounds to the skin. Regarding the LN formulations, LN-F1 released a superior amount of phenolic compounds, followed by LN-F2 and LN-F3. Moreover, a rapid release of lemon polyphenols from the LN was observed, possibly due to increased surface area of the fabricated nanodroplets that permeated easily through the dialysis membranes. Furthermore, since the LN droplet size was found to be smaller than 200 nm, it might enhance the solubility of phenolic compounds, as reported previously [54]. Also, as corroborated by the rheology results, as the concentration of xanthan gum increases, the viscosity rises while the release capacity of the formulation decreases. In this way, the higher viscosity of the LN formulation, which is also related to lower water content, may result in slower diffusion of the phenolic compounds, which is in agreement with previous studies [55]. In addition, the in vitro release profiles were treated with different mathematical models. Thus, the release pattern of phenolic compounds from all LN formulations and from LE followed the Higuchi equation, as indicated by the highest correlation coefficient ( $R^2$ ). The Higuchi model, in conjunction with the Korsmeyers–Peppas model, suggested a non-Fickian diffusion release from the gel matrix,

in accordance with other published results for the same delivery system [56]. Therefore, the advantages of a delivery system through a nanoemulgel include good adhesion to the skin surface and high delivery capacity leading to a larger concentration gradient of bioactive compounds [57].

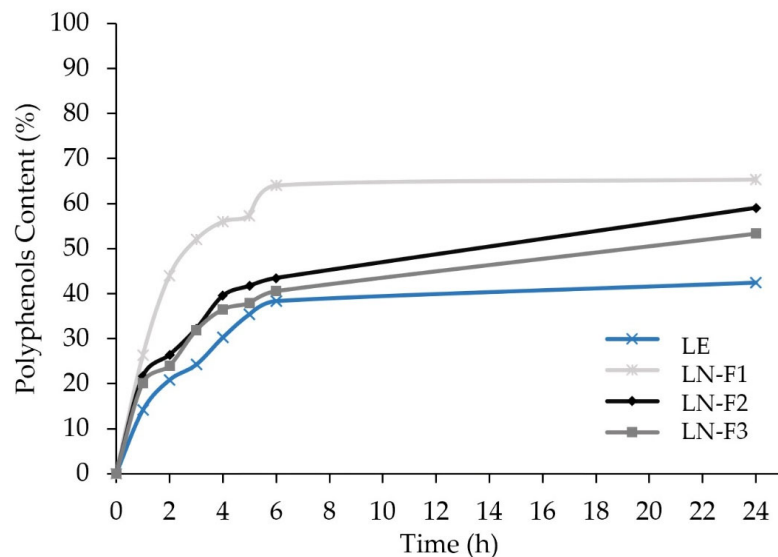


**Figure 5.** In vitro polyphenolic content release profile of the lemon-extract-based nanoemulgel formulations (LN-F1, LN-F2, and LN-F3) and the free lemon extract (LE).

### 3.5. LN Optimal Formulation Selection and Characterization

Considering all the abovementioned results, LN-F2 was selected as the optimal formulation due to improved physicochemical characteristics and favorable in vitro release capacity. Therefore, LN-F1 and LN-F3 were excluded from additional analysis, while LN-F2 was further characterized and evaluated for potential bioactivities.

#### 3.5.1. Phenolic Content Analysis

To corroborate the previous analysis, the optimal selected formulation (LN-F2) was assessed for the identification and quantification of phenolic compounds. Therefore, according to the obtained results (Table 3 and Figure 6) 12 phenolic compounds were identified within this formulation, with narirutin ( $195.000 \pm 0.670 \mu\text{g/g}$ ), naringenin ( $160.000 \pm 0.803 \mu\text{g/g}$ ), hesperidin ( $74.000 \pm 0.410 \mu\text{g/g}$ ), chlorogenic acid ( $9.530 \pm 0.510 \mu\text{g/g}$ ), diosmine ( $4.830 \pm 0.030 \mu\text{g/g}$ ), and coumaric acid ( $2.540 \pm 0.010 \mu\text{g/g}$ ) being the ones in major quantities. Although in lower concentrations, ellagic and ferulic acids, rutin, hesperetin, and methyl gallate were also identified. The concentration of each phenolic compound can vary depending on the lemon variety. Nonetheless, the obtained concentrations are in accordance with the values described in the literature for lemon extracts [53,58]. Furthermore, several of the identified compounds, such as naringenin, hesperidin, ellagic acid, and coumaric acid, are commonly found in *Citrus* species and have been researched for their antioxidant, anti-inflammatory, antimicrobial, and antiviral activities [31,59–61]. Therefore, besides LN-F2 being capable of maintaining the integrity of polyphenolic compounds after formulation, it presented promising results regarding the identified and quantified compounds due to their potential bioactivities.

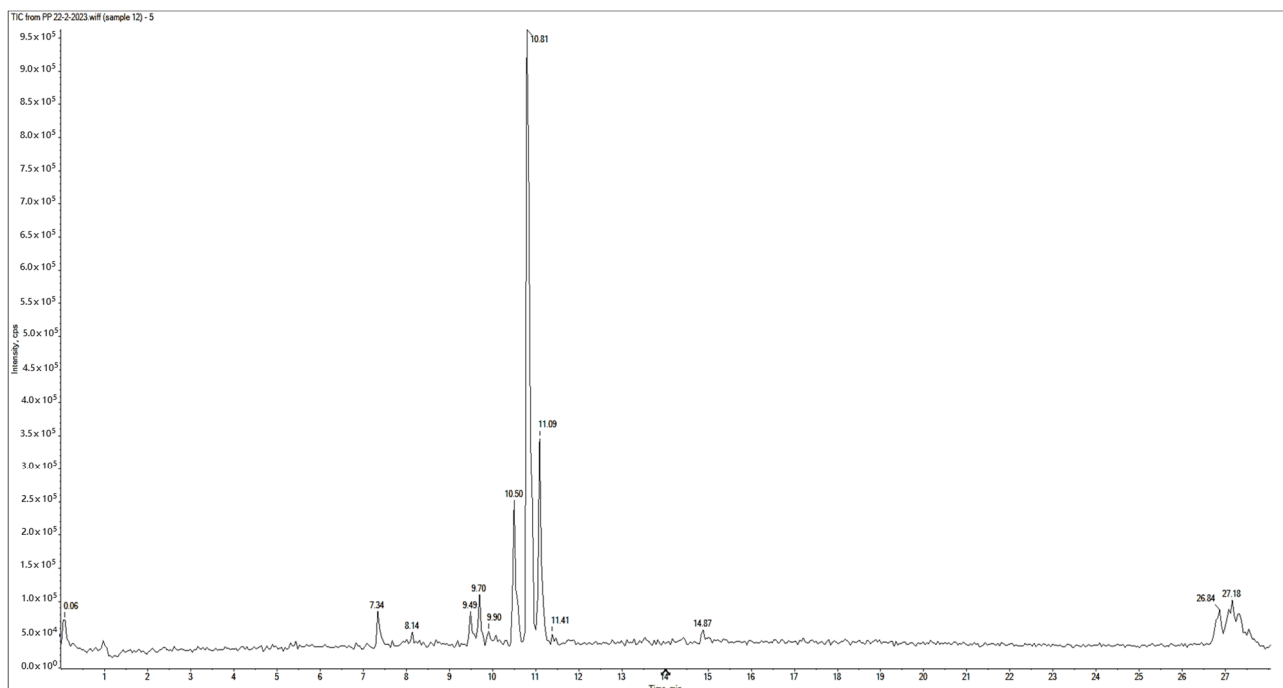
#### 3.5.2. TEM Characterization

A TEM characterization was carried out to analyze the morphology of LN-F2. The micrograph (Figure 7) revealed that droplets were spherical and corroborated that the average droplet size was less than 200 nm, being within the nanosize range [47]. Therefore, these results validate that the developed formulation can be defined as a nanoemulsion. Moreover, the TEM micrograph results align with the aforementioned size determination values.

**Table 3.** Identification and quantification ( $\mu\text{g/g}$ ) of the phenolic compounds present in the selected nanoemulgel formulation (LN-F2).

Phenolic Compound	Calibration Curve Equation	$R^2$	LOD (ng/mL)	LOQ (ng/mL)	Rt (min)	Concentration $\pm$ SD ( $\mu\text{g/g}$ )
Narirutin	$y = -0.002538650 + 0.0256495x$	0.9998	10.25	20.01	10.84	$195.000 \pm 0.670$
Naringenin	$y = -0.000761480 + 0.0310687x$	0.9996	12.31	23.57	15.02	$160.320 \pm 0.803$
Hesperidin	$y = 0.000321812 + 0.00008838x$	0.9997	15.41	30.19	11.10	$74.000 \pm 0.410$
Chlorogenic acid	$y = -0.000162510 + 0.0082195x$	0.9993	21.84	30.84	8.13	$9.530 \pm 0.510$
Diosmin	$y = -0.040602700 + 0.1132100x$	0.9997	15.10	30.62	11.03	$4.830 \pm 0.030$
Coumaric acid	$y = -0.000916311 + 0.0643206x$	0.9995	15.03	30.58	9.75	$2.540 \pm 0.010$
Rutin	$y = -0.002097290 + 0.0613716x$	0.9998	15.06	30.37	9.91	$1.490 \pm 0.009$
Ellagic acid	$y = -0.000728175 + 0.0480413x$	0.9996	15.14	30.89	10.12	$1.200 \pm 0.002$
Ferulic acid	$y = -0.000938050 + 0.0189100x$	0.9987	14.98	30.97	10.38	$1.170 \pm 0.006$
Saponarin	$y = 0.001245340 + 0.0568465x$	0.9993	15.54	30.47	8.66	$0.420 \pm 0.004$
Hesperetin	$y = 0.000213181 + 0.0007883x$	0.9996	15.41	30.12	15.56	$0.210 \pm 0.001$
Methyl gallate	$y = -0.001515260 + 0.0801915x$	0.9998	15.78	40.21	7.65	$0.120 \pm 0.001$

$R^2$ , correlation coefficient; LOD, limit of detection; LOQ, limit of quantification; Rt, retention time.

**Figure 6.** Chromatogram of the selected optimal nanoemulgel formulation (LN-F2).

### 3.5.3. Cytotoxicity Assessment on MA-104 Cells

To assess the potential cytotoxic effect of LE and LN-F2, MA-104 cells were exposed to several concentrations of each sample (ranging from  $10 \mu\text{g}/100 \text{ mL}$  to  $1 \text{ mg}/100 \mu\text{L}$ ), and their morphology was continually evaluated by inverted light microscopy [23]. According to the results obtained through this test, no morphological alterations, such as loss of confluence, cell rounding and shrinking, cytoplasm granulation, and/or vacuolization, were observed in the tested cells for up to 72 h and at the concentrations of LE and LN-F2 that were applied. Furthermore, as mentioned by Diab et al. [59], who tested the effect of lemon extract (300, 200, and  $500 \mu\text{g}/\text{mL}$ ) on mouse splenocytes, no cytotoxic effects were reported, and even proliferative activity was observed in these cells after treatment. Moreover, the results also suggest that the LN matrix did not have a cytotoxic effect on MA-104 under the tested conditions.

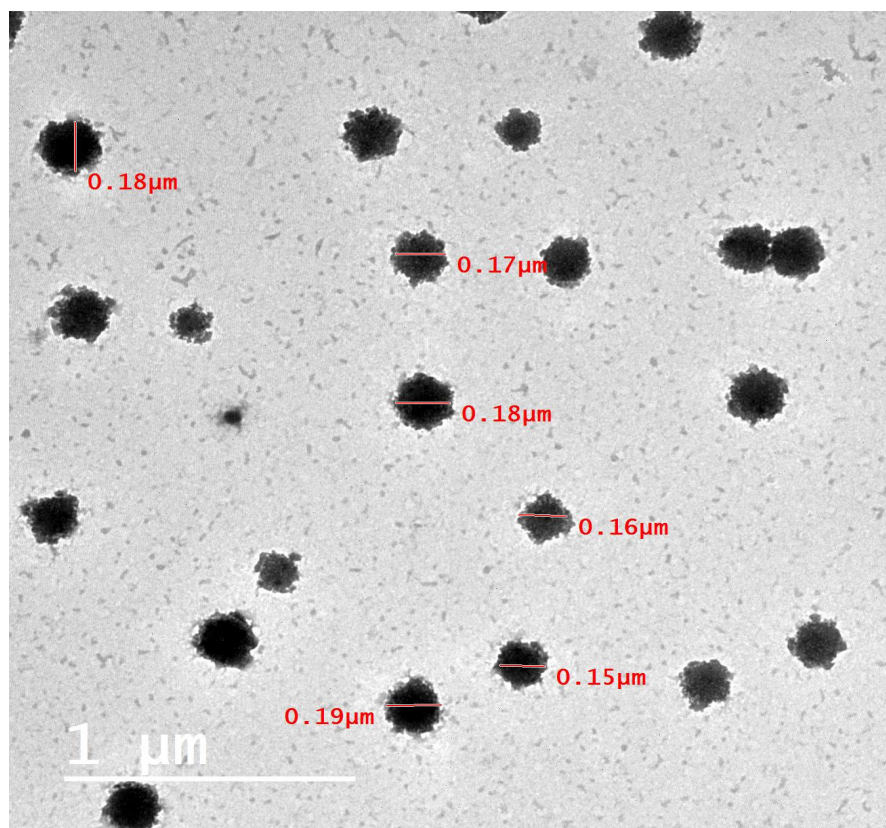


**Figure 7.** TEM micrograph of the selected optimal nanoemulgel formulation (LN-F2).

### 3.6. Bioactivity Analyses

#### 3.6.1. LE and LN-F2 Antiviral Activity

After 30 min and 60 min of incubation, both LE and LN-F2 did not show any antiviral activity against rotavirus (SA-11). However, when tested against phiX 174 virus, after 30 min, both samples promote a final viral count reduction at concentrations of 10 mg/mL (Figure 8). Furthermore, LE at a concentration of 10 mg/mL showed a 22.58% virus reduction, while the LN-F2 containing 1 mg/mL or 10 mg/mL of LE showed a 3.23% and 24.19% reduction of phiX 174 infection, respectively. Therefore, these results suggest that, at the same LE concentration, the antiviral efficiency is similar for free LE and LE formulated into the nanoemulgel (LN-F2). Moreover, the results also suggest that the antiviral effectiveness of the LN-F2 is dose-dependent.

The results obtained for the phiX 174 bacteriophage are corroborated by previous results on this matter, since many studies have proved the activity of *Citrus* extracts against other types of viruses such as SARS-CoV-2 [62], HSV-1 [63], and Lassa virus [64]. These results might be related to the presence of bioactive compounds such as phenolic compounds (e.g., hesperidin or tangeritin) within the lemon extract, since they have been reported to have antiviral activity against different viruses [50,64]. One of the mechanisms for this bioactivity was described by Tang et al. [64], who stated that these types of extracts might be able to block the entry of the virus into the cell at the viral fusion step. Additionally, as already mentioned, it is important to consider that the extracts' bioactivities on certain pathogens might depend on the plant composition from where the extract is obtained. Furthermore, this composition varies according to several factors such as climatic and growing conditions. Nonetheless, to the best of our knowledge, this is the first report on the in vitro antiviral activity of a nanoemulgel formulation containing lemon peel extract against phiX 174.

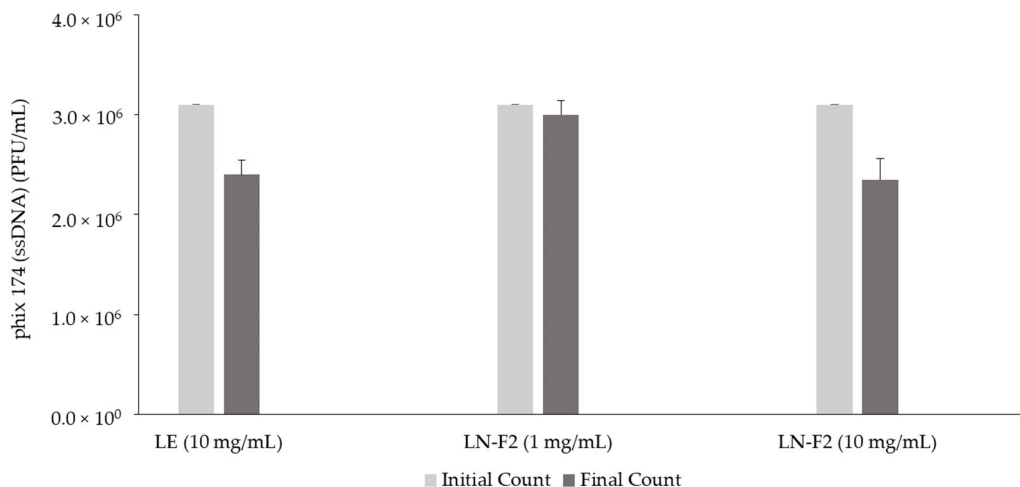


**Figure 8.** Viral counts of phiX 174 (ssDNA) before (initial) and after (final) exposure to 10 mg/mL of lemon extract (LN) and 1 mg/mL or 10 mg/mL of the selected optimal nanoemulgel formulation (LN-F2), for 30 min, at 37 °C. The results are presented in plaque-forming units (PFU)/mL and as mean  $\pm$  SD.

### 3.6.2. LN-F2 In Vitro Antimicrobial Activity

To corroborate the previous antimicrobial results of LE and to assess if the extract retains this bioactivity after its formulation into the nanoemulgel matrix, the antimicrobial activity of LN-F2 was evaluated by well and disk diffusion assays. This test was carried out against two Gram-positive bacterial strains: *Staphylococcus aureus* and *Listeria monocytogenes*; three Gram-negative bacterial strains: *Escherichia coli*, *Salmonella enterica* serovar Typhimurium, *Pseudomonas aeruginosa*; and a yeast: *Candida albicans*. As shown in Figure 9, LN-F2 exhibited in vitro antimicrobial activity against all six pathogenic microorganisms by both well and disk diffusion methods, consistent with the MIC/MMC results previously obtained. Also, it was observed that the zones of inhibition (ZIs) achieved by using the well diffusion method were slightly larger than those obtained using the disk diffusion method. Moreover, it can be observed that, regarding both methods, the most affected microorganism was *E. coli*, with ZIs of 11 mm and 10 mm for the well and disk techniques, respectively. On the other hand, concerning only the well diffusion method, the effect against *Candida albicans* was the lowest, resulting in a ZI of 8 mm, while for the disk diffusion method the least affected microorganisms were *S. Typhimurium*, *P. aeruginosa*, *S. aureus*, and *C. albicans*, all of which presented a ZI of 8 mm. Overall, LN-F2 seems to exhibit similar effects against the tested microorganisms. Once again, this activity might be mainly related to the lemon peel extract components such as the major phenolic compounds found and natural organic acids such as ascorbic and citric acids, which have demonstrated great antimicrobial properties [65]. Therefore, several studies show that extracts obtained from the lemon peel exhibited antimicrobial properties against *Salmonella* Typhimurium, *Bacillus cereus*, *Listeria monocytogenes*, *E. coli*, and *Enterococcus faecalis* [66–68]. Moreover, xanthan gum has shown a synergistic effect and enhancement of the antioxidant and antimicrobial activity of the lemon peel extract against microbial pathogens. In addition, xanthan gum increases the thickness, stability, as well as moisture content of the gel due to the presence of -OH groups, which increase the formation of hydrogen bonds [65,69], aiding in overall extract stabilization and bioactive capacities. Although the antimicrobial capacity of lemon extracts has not been studied within a nanoemulgel formulation, a work carried out by Yabalak et al. [70] described that the MICs of *Citrus*-essential-oil-incorporating gelatine film solution against *E. coli* and *S. aureus* were about 10.1 and 9.1 mg/mL, respectively. Hence, as far as it is concerned, this is the first study where a nanoemulgel formulation based on *Citrus limon* peel extract showed antimicrobial activity against Gram-positive and Gram-negative bacteria and fungi.

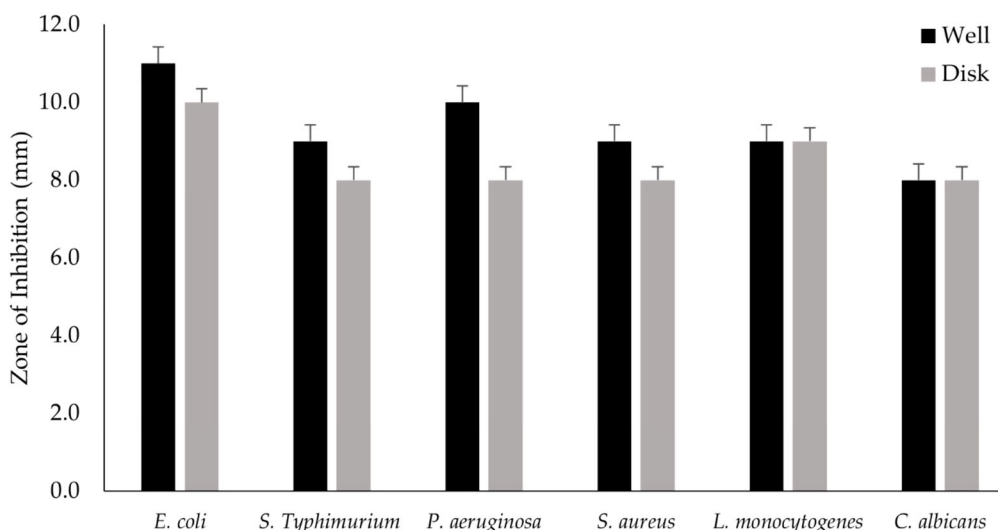


**Figure 9.** Zones of inhibition (mm) obtained by LN-F2 against *E. coli*, *S. enterica* serovar Typhimurium, *P. aeruginosa*, *S. aureus*, *L. monocytogenes*, and *C. albicans* by well and disk diffusion methods.

### 3.6.3. LN-F2 In Vivo Antimicrobial Activity

To assess the in vivo antimicrobial capacity of the formulated nanoemulgel, the hands of 20 volunteers were analyzed for the presence and quantity of bacteria and fungi, before and after the application of the LN-F2. Prior to the usage of LN-F2, the lowest total microbial count was 50 CFU/cm<sup>2</sup> for bacteria and 5 CFU/cm<sup>2</sup> for fungi, while the highest values for bacterial and fungal counts were 1500 CFU/cm<sup>2</sup> and 580 CFU/cm<sup>2</sup>, respectively. Moreover, 3 out of 20 samples were free from any fungi before the application of the nanoemulgel (Table 4). After using LN-F2, the findings demonstrated that the formulated nanoemulgel has strong in vivo antimicrobial activity against the tested bacteria and fungus, promoting efficient removal of these microorganisms from the volunteers' hands (Figures 10 and 11). The average percentage of total bacterial counts removed (R %) from all samples was 95.11 ± 4.41%. Additionally, the average removal percentage of the total fungal counts was 97.01 ± 3.75. Therefore, it can be concluded that LN-F2, containing lemon peel extract, seems to have strong in vivo antimicrobial activity, which is in accordance with the previous analysis. Moreover, regarding the antifungal activity, these results are also corroborated by the findings reported in the literature that mention, for instance, the capacity of lemon extract to counteract *Alternaria* spp., *Curvularia* spp., *Fusarium* spp., *Trichophyton* spp., and *Geotrichum* spp. [71].

**Table 4.** Total bacterial and fungal counts in the microbial suspension samples collected from the volunteers' hands before and after the application of LN-F2.

Volunteer ID	Age	Gender	Total Bacterial Counts (CFU/cm <sup>2</sup> )		R%	Total Fungal Counts (CFU/cm <sup>2</sup> )		R%
			Before	After		Before	After	
1	39	M	1200	100	91.66	95	3	94.96
2	30	M	850	20	97.47	20	0	100.00
3	44	M	190	10	94.73	10	0	100.00
4	43	M	130	0	100.00	5	0	100.00
5	25	F	200	5	97.50	0	0	N/A
6	35	M	1100	120	89.09	100	9	91.00
7	40	M	500	30	94.00	150	0	100.00
8	41	M	90	0	100.00	12	0	100.00
9	39	F	420	30	92.85	190	4	97.89

**Table 4.** Cont.

Volunteer ID	Age	Gender	Total Bacterial Counts (CFU/cm <sup>2</sup> )		R%	Total Fungal Counts (CFU/cm <sup>2</sup> )		R%
			Before	After		Before	After	
10	26	M	1000	105	98.50	580	60	89.65
11	32	M	1500	250	83.33	120	10	91.66
12	38	F	750	45	94.00	35	0	100.00
13	48	M	60	0	100.00	0	0	N/A
14	67	M	250	10	96.00	18	0	100.00
15	65	M	690	55	92.02	90	5	94.44
16	44	M	500	40	92.00	150	10	93.33
17	30	M	990	30	96.96	80	3	96.25
18	39	M	250	20	92.00	30	0	100.00
19	43	M	120	0	100.00	0	0	N/A
20	30	M	50	0	100.00	20	0	100.00
Average ± SD	-	-	-	-	95.11 ± 4.41	-	-	97.01 ± 3.75

M, male; F, female; CFU, colony-forming unit; R%, removal percentage; N/A, not applicable.

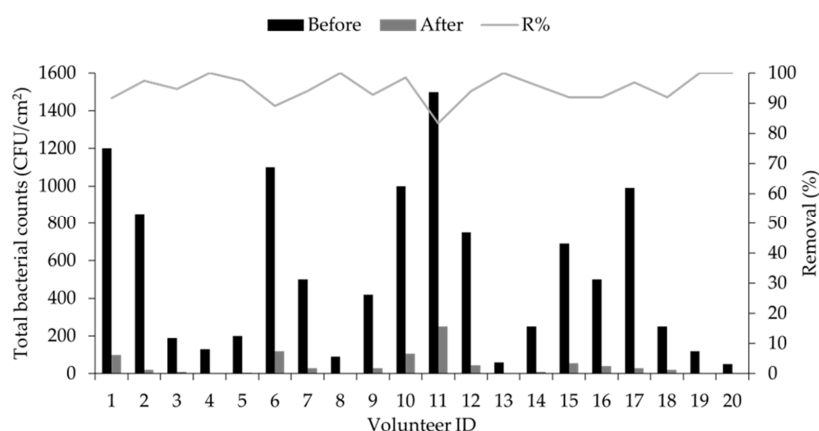


**Figure 10.** Total bacterial counts before and after the application of LN-F2 on volunteers' hands and the respective removal percentage (R%).

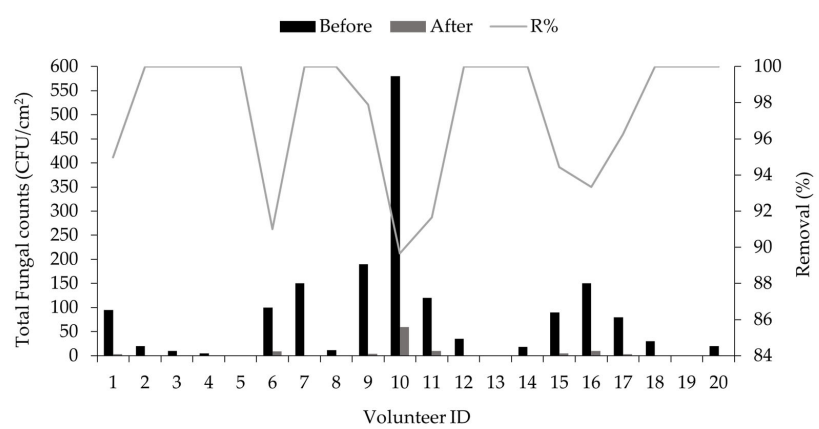


**Figure 11.** Total fungal counts before and after the application of LN-F2 on volunteers' hands and the respective removal percentage (R%).

Furthermore, following the completion of this assessment, there were no indications of irritation, dermal abrasion, trauma, or infection observed within or around the area of the formulation application. Additionally, the volunteers did not report any potential side effects after the application of the formulation.

#### 4. Conclusions

The present study aimed to develop and characterize an alcohol-free lemon-peel-extract-based nanoemulgel for hand-sanitizing purposes. In conclusion, the lemon peel extract (LE) presented antimicrobial activity against various microorganisms, including *S. aureus*, *E. coli*, and *C. albicans*, with relatively low MIC values. Also, the correlation between MIC and MMC values further highlighted the extract's consistent antimicrobial activity across the different strains.

Moreover, three different nanoemulgels (LN-F1, LN-F2, and LN-F3) were developed using LE, with a focus on creating an optimal formulation for potential hand-sanitizing applications. The formulations exhibited satisfactory macroscopic characteristics, and the FTIR spectra indicated successful incorporation of LE without significant alterations to its chemical structure. In addition, the nanoemulsion's particle size, polydispersity index, zeta potential, and pH values met the criteria for stability. However, LN-F2 emerged as the optimal formulation based on stability under extreme conditions, rheological behavior, and effective in vitro release of phenolic compounds. Furthermore, the characterization of LN-F2 revealed the presence of bioactive compounds, the major ones being naringin, naringenin, hesperidin, and chlorogenic acid. LN-F2 also exhibited promising results in terms of safety, with no cytotoxic effects observed on MA-104 cells at the tested concentrations. In antiviral assays, both LE and LN-F2 did not affect rotavirus SA-11 but were able to induce the reduction of phiX 174 virus. Additionally, LN-F2 demonstrated in vitro antimicrobial activity against various pathogenic microorganisms, aligning with the LE MIC/MMC results. Also, the in vivo antimicrobial efficacy of LN-F2 was validated through the assessment of its efficacy against microorganisms present on the volunteers' hands, revealing substantial reductions in bacterial and fungal counts after application. Therefore, the strong antimicrobial activity of LN-F2, both in vitro and in vivo, suggests its potential as an effective hand-sanitizing formulation.

Overall, this work provides comprehensive insights into the antimicrobial and formulation aspects of lemon peel extract, highlighting its enhanced potential for applications in the fields of antimicrobial and antiviral formulations, particularly when incorporated into advanced delivery systems such as nanoemulgel matrices.

**Author Contributions:** Conceptualization, F.M.I., E.S.S. and E.S.E.H.; methodology, F.M.I., R.S.M., E.S.S., M.A.E.-L. and S.A.-E.; validation, F.M.I., R.S.M., E.S.S., M.A.E.-L. and S.A.-E.; formal analysis, F.M.I.; investigation, F.M.I., R.S.M., E.S.S., M.A.E.-L., S.I.S. and S.A.-E.; resources, F.M.I., R.S.M., E.S.S., M.A.E.-L. and S.A.-E.; data curation, F.M.I., R.S.M., E.S.S., M.A.E.-L., S.A.-E. and C.V.R.; writing—original draft preparation, F.M.I., R.S.M., E.S.S., M.A.E.-L. and S.A.-E.; writing—review and editing, F.M.I., C.V.R. and M.P.; visualization, F.M.I.; supervision, E.S.E.H.; project administration, E.S.E.H.; funding acquisition, E.S.E.H. All authors have read and agreed to the published version of the manuscript.

**Funding:** The development of the present work was supported by the MEDISMART project Mediterranean Citrus innovative soft processing solutions for S.M.A.R.T (Sustainable, Mediterranean, Agronomically evolved nutritionally enriched Traditional) products (reference number: 2019-SECTION2), and through the Science, Technology and Innovation Funding Authority (STDF), Egypt, and Portuguese national funds from Fundação para a Ciência e Tecnologia (FCT) (reference: DOI 10.54499/PRIMA/0014/2019).

**Institutional Review Board Statement:** The study was conducted in accordance with the Declaration of Helsinki and approved by the National Research Center's Ethics and Animal Care Committee (Ethic No. 20236).

**Informed Consent Statement:** Informed consent was obtained from all subjects involved in the study.

**Data Availability Statement:** The data generated and/or analyzed during the current study are available from the corresponding author on reasonable request.

**Acknowledgments:** The authors acknowledge the MEDISMART project (reference number: 2019-SECTION2), Science, Technology and Innovation Funding Authority (STDF), Egypt, and Fundação para a Ciência e Tecnologia (FCT) (reference: DOI 10.54499/PRIMA/0014/2019) for the

financial assistance provided. Furthermore, the authors extend their appreciation for the scientific collaboration with CBQF within the framework of the UIDB/50016/2020 project.

**Conflicts of Interest:** The authors declare no conflicts of interest.

## References

- Golin, A.P.; Choi, D.; Ghahary, A. Hand sanitizers: A review of ingredients, mechanisms of action, modes of delivery, and efficacy against coronaviruses. *Am. J. Infect. Control* **2020**, *48*, 1062–1067. [CrossRef] [PubMed]
- Saha, T.; Khadka, P.; Das, S.C. Alcohol-based hand sanitizer—composition, proper use and precautions. *Germs* **2021**, *11*, 408–417. [CrossRef] [PubMed]
- Hamad Vuai, S.A.; Sahini, M.G.; Sule, K.S.; Ripanda, A.S.; Mwanga, H.M. A comparative in-vitro study on antimicrobial efficacy of on-market alcohol-based hand washing sanitizers towards combating microbes and its application in combating COVID-19 global outbreak. *Heliyon* **2022**, *8*, e11689. [CrossRef] [PubMed]
- Ibrahim, F.M.; Mohammed, R.S.; Abdelsalam, E.; Ashour, W.E.; Magalhães, D.; Pintado, M.; El Habbasha, E.S. Egyptian Citrus Essential Oils Recovered from Lemon, Orange, and Mandarin Peels: Phytochemical and Biological Value. *Horticulturae* **2024**, *10*, 180. [CrossRef]
- Vilas-Boas, A.A.; Magalhães, D.; Campos, D.A.; Porretta, S.; Dellapina, G.; Poli, G.; Istanbullu, Y.; Demir, S.; San Martín, Á.M.; García-Gómez, P.; et al. Innovative Processing Technologies to Develop a New Segment of Functional Citrus-Based Beverages: Current and Future Trends. *Foods* **2022**, *11*, 3859. [CrossRef] [PubMed]
- Vilas Boas, A.; Gómez-García, R.; Campos, D.; Correia, M.; Pintado, M. Integrated Biorefinery Strategy for Orange Juice By-products Valorization: A Sustainable Protocol to Obtain Bioactive Compounds. In *Food Waste Conversion; Methods and Protocols in Food Science*; Humana: New York, NY, USA, 2023; pp. 113–124.
- Shri Balakrishna, A.; Saradindu, G.; Giriraj, Y.; Kavita, S.; Sirsendu, G.; Sushil, J. Formulation, Evaluation and Antibacterial Efficiency of water-based herbal Hand Sanitizer Gel. *bioRxiv* **2018**, 373928. [CrossRef]
- Rodrigues, C.V.; Pintado, M. Hesperidin from Orange Peel as a Promising Skincare Bioactive: An Overview. *Int. J. Mol. Sci.* **2024**, *25*, 1890. [CrossRef] [PubMed]
- Liu, Y.; Benohoud, M.; Galani Yamdeu, J.H.; Gong, Y.Y.; Orfila, C. Green extraction of polyphenols from citrus peel by-products and their antifungal activity against Aspergillus flavus. *Food Chem. X* **2021**, *12*, 100144. [CrossRef]
- Choudhury, H.; Gorain, B.; Pandey, M.; Chatterjee, L.A.; Sengupta, P.; Das, A.; Molugulu, N.; Kesharwani, P. Recent Update on Nanoemulgel as Topical Drug Delivery System. *J. Pharm. Sci.* **2017**, *106*, 1736–1751. [CrossRef]
- Algahtani, M.S.; Ahmad, M.Z.; Ahmad, J. Nanoemulgel for Improved Topical Delivery of Retinyl Palmitate: Formulation Design and Stability Evaluation. *Nanomaterials* **2020**, *10*, 848. [CrossRef]
- Bashir, M.; Ahmad, J.; Asif, M.; Khan, S.U.; Irfan, M.; Ibrahim, A.Y.; Asghar, S.; Khan, I.U.; Iqbal, M.S.; Haseeb, A.; et al. Nanoemulgel, an Innovative Carrier for Diflunisal Topical Delivery with Profound Anti-Inflammatory Effect: In vitro and in vivo Evaluation. *Int. J. Nanomed.* **2021**, *16*, 1457–1472. [CrossRef] [PubMed]
- Morsy, M.A.; Abdel-Latif, R.G.; Nair, A.B.; Venugopala, K.N.; Ahmed, A.F.; Elsewedy, H.S.; Shehata, T.M. Preparation and evaluation of atorvastatin-loaded nanoemulgel on wound-healing efficacy. *Pharmaceutics* **2019**, *11*, 609. [CrossRef] [PubMed]
- Asfour, M.H.; Mohsen, A.M. Formulation and evaluation of pH-sensitive rutin nanospheres against colon carcinoma using HCT-116 cell line. *J. Adv. Res.* **2018**, *9*, 17–26. [CrossRef]
- Elhabak, M.; Ibrahim, S.; Abouelatta, S.M. Topical delivery of l-ascorbic acid spanlastics for stability enhancement and treatment of UVB induced damaged skin. *Drug Deliv.* **2021**, *28*, 445–453. [CrossRef]
- Chellappa, P.; Eid, A.M.; Elmarzugi, N. Preparation and characterization of virgin coconut oil nanoemulgel. *J. Chem. Pharm. Res.* **2015**, *7*, 787–793.
- Srivastava, M.; Kohli, K.; Ali, M. Formulation development of novel in situ nanoemulgel (NEG) of ketoprofen for the treatment of periodontitis. *Drug Deliv.* **2016**, *23*, 154–166. [CrossRef]
- Sohail, M.; Naveed, A.; Abdul, R.; Khan, H.M.S.; Khan, H. An approach to enhanced stability: Formulation and characterization of Solanum lycopersicum derived lycopene based topical emulgel. *Saudi Pharm. J.* **2018**, *26*, 1170–1177. [CrossRef] [PubMed]
- Mostafa, D.M.; Abd El-Alim, S.H.; Asfour, M.H.; Al-Okbi, S.Y.; Mohamed, D.A.; Hamed, T.E.-S.; Awad, G. Transdermal fennel essential oil nanoemulsions with promising hepatic dysfunction healing effect: In vitro and in vivo study. *Pharm. Dev. Technol.* **2019**, *24*, 729–738. [CrossRef]
- Abd El-Alim, S.H.; Salama, A.; Darwish, A.B. Provesicular elastic carriers of Simvastatin for enhanced wound healing activity: An in-vitro/in-vivo study. *Int. J. Pharm.* **2020**, *585*, 119470. [CrossRef]
- Zhang, X.; Liu, D.; Jin, T.Z.; Chen, W.; He, Q.; Zou, Z.; Zhao, H.; Ye, X.; Guo, M. Preparation and characterization of gellan gum-chitosan polyelectrolyte complex films with the incorporation of thyme essential oil nanoemulsion. *Food Hydrocoll.* **2021**, *114*, 106570. [CrossRef]
- Ammar, N.M.; Hassan, H.A.; Mohammed, M.A.; Serag, A.; Abd El-Alim, S.H.; Elmotasem, H.; El Raey, M.; El Gendy, A.N.; Sobeh, M.; Abdel-Hamid, A.-H.Z. Metabolomic profiling to reveal the therapeutic potency of Posidonia oceanica nanoparticles in diabetic rats. *RSC Adv.* **2021**, *11*, 8398–8410. [CrossRef] [PubMed]

23. Wu, S.; Zeng, L.; Wang, C.; Yang, Y.; Zhou, W.; Li, F.; Tan, Z. Assessment of the cytotoxicity of ionic liquids on Spodoptera frugiperda 9 (Sf-9) cell lines via in vitro assays. *J. Hazard. Mater.* **2018**, *348*, 1–9. [CrossRef] [PubMed]
24. England, P.H. *Detection and Enumeration of Bacteria in Swabs and Other Environmental Samples*, 4th ed.; Volume National Infection Service, Food, Water and Environmental Microbiology Standard Method FNES4 (E1): London, UK, 2017; p. 22.
25. Aa, L.; Is, H.; Jh, D.; Jfr, L. Bacterial contamination of the hands of food handlers as indicator of hand washing efficacy in some convenient food industries. *Pak. J. Med. Sci.* **2014**, *30*, 755–758. [PubMed]
26. Rice, E.W.; Bridgewater, L.; Association, A.P.H. *Standard Methods for the Examination of Water and Wastewater*; American Public Health Association: Washington, DC, USA, 2012; Volume 10.
27. Elwakeel, K.Z.; El-Liethy, M.A.; Ahmed, M.S.; Ezzat, S.M.; Kamel, M.M. Facile synthesis of magnetic disinfectant immobilized with silver ions for water pathogenic microorganism's deactivation. *Environ. Sci. Pollut. Res. Int.* **2018**, *25*, 22797–22809. [CrossRef] [PubMed]
28. Magréault, S.; Jauréguy, F.; Carbonnelle, E.; Zahar, J.R. When and How to Use MIC in Clinical Practice? *Antibiotics* **2022**, *11*, 1748. [CrossRef] [PubMed]
29. Parvekar, P.; Palaskar, J.; Metgud, S.; Maria, R.; Dutta, S. The minimum inhibitory concentration (MIC) and minimum bactericidal concentration (MBC) of silver nanoparticles against *Staphylococcus aureus*. *Biomater. Investigig. Dent.* **2020**, *7*, 105–109. [CrossRef] [PubMed]
30. Otang, W.M.; Afolayan, A.J. Antimicrobial and antioxidant efficacy of *Citrus limon* L. peel extracts used for skin diseases by Xhosa tribe of Amathole District, Eastern Cape, South Africa. *S. Afr. J. Bot.* **2016**, *102*, 46–49. [CrossRef]
31. Henderson, A.H.; Fachrial, E.; Lister, I.N.E. Antimicrobial Activity of Lemon (*Citrus limon*) Peel Extract Against Escherichia coli. *Am. Sci. Res. J. Eng. Technol. Sci.* **2018**, *39*, 268–273.
32. John, S.; Monica, S.; Priyadarshini, S.; Sivaraj, C.; Arumugam, P. Antioxidant and antimicrobial activity of lemon peel. *Int. J. Pharm. Sci. Rev. Res.* **2017**, *46*, 115–118.
33. Saleem, M.; Durani, A.I.; Asari, A.; Ahmed, M.; Ahmad, M.; Yousaf, N.; Muddassar, M. Investigation of antioxidant and antibacterial effects of citrus fruits peels extracts using different extracting agents: Phytochemical analysis with in silico studies. *Heliyon* **2023**, *9*, e15433. [CrossRef]
34. Shanmugam, R.; Lakki Reddy Venkata, B.R.; Geetha, R.V. Broad spectrum antibacterial silver nanoparticle green synthesis: Characterization, and mechanism of action. In *Green Synthesis, Characterization and Applications of Nanoparticles*; Elsevier: Amsterdam, The Netherlands, 2019; pp. 429–444.
35. Karaman, R.; Jubeh, B.; Breijeh, Z. Resistance of Gram-Positive Bacteria to Current Antibacterial Agents and Overcoming Approaches. *Molecules* **2020**, *25*, 2888. [CrossRef] [PubMed]
36. Hamida, R.S.; Ali, M.A.; Goda, D.A.; Khalil, M.I.; Al-Zaban, M.I. Novel Biogenic Silver Nanoparticle-Induced Reactive Oxygen Species Inhibit the Biofilm Formation and Virulence Activities of Methicillin-Resistant *Staphylococcus aureus* (MRSA) Strain. *Front. Bioeng. Biotechnol.* **2020**, *8*, 433. [CrossRef] [PubMed]
37. Qiu, C.; Zhao, M.; McClements, D. Improving the stability of wheat protein-stabilized emulsions: Effect of pectin and xanthan gum addition. *Food Hydrocoll.* **2015**, *43*, 377–387. [CrossRef]
38. Mulia, K.; Ramadhan, R.M.A.; Krisanti, E.A.J.M.W.C. Formulation and characterization of nanoemulgel mangosteen extract in virgin coconut oil for topical formulation. *MATEC Web. Conf.* **2018**, *156*, 01013. [CrossRef]
39. Matman, N.; Min Oo, Y.; Amnuaikit, T.; Somnuk, K. Continuous production of nanoemulsion for skincare product using a 3D-printed rotor-stator hydrodynamic cavitation reactor. *Ultrason. Sonochemistry* **2022**, *83*, 105926. [CrossRef] [PubMed]
40. Semalty, A.; Semalty, M.; Singh, D.; Rawat, M. Preparation and characterization of phospholipid complexes of naringenin for effective drug delivery. *J. Incl. Phenom. Macrocycl. Chem.* **2010**, *67*, 253–260. [CrossRef]
41. Thombare, N.; Mahto, A.; Singh, D.; Roy Chowdhury, A.; Ansari, M. Comparative FTIR Characterization of Various Natural Gums: A Criterion for Their Identification. *J. Polym. Environ.* **2023**, *31*, 3372–3380. [CrossRef]
42. Rehman, M.; Rasul, A.; Khan, M.; Hanif, M.; Naeem Aamir, M.; Khan, H.m.; Hameed, M.; Akram, M. Development of niosomal formulations loaded with cyclosporine A and evaluation of its compatibility. *Trop. J. Pharm. Res.* **2018**, *17*, 1457–1464. [CrossRef]
43. Kondiah, P.P.D.; Rants'o, T.A.; Mdanda, S.; Mohlomi, L.M.; Choonara, Y.E. A Poly (Caprolactone)-Cellulose Nanocomposite Hydrogel for Transdermal Delivery of Hydrocortisone in Treating Psoriasis Vulgaris. *Polymers* **2022**, *14*, 2633. [CrossRef]
44. Kanaze, F.; Kokkalou, E.; Niopas, I.; Georgarakis, M.; Stergiou, A.; Bikaris, D. Thermalanalysis study of flavonoid solid dispersions having enhanced solubility. *J. Therm. Anal. Calorim.* **2006**, *83*, 283–290. [CrossRef]
45. Mushtaq, A.; Mohd Wani, S.; Malik, A.R.; Gull, A.; Ramniwas, S.; Ahmad Nayik, G.; Ercisli, S.; Alina Marc, R.; Ullah, R.; Bari, A. Recent insights into Nanoemulsions: Their preparation, properties and applications. *Food Chem. X* **2023**, *18*, 100684. [CrossRef] [PubMed]
46. Verdú-Soriano, J.; Casado-Díaz, A.; de Cristino-Espinar, M.; Luna-Morales, S.; Dios-Guerra, C.; Moreno-Moreno, P.; Dorado, G.; Quesada-Gómez, J.M.; Rodríguez-Mañas, L.; Lázaro-Martínez, J.L. Hard-to-Heal Wound Healing: Superiority of Hydrogel EHO-85 (Containing Olea europaea Leaf Extract) vs. a Standard Hydrogel. A Randomized Controlled Trial. *Gels* **2023**, *9*, 962. [CrossRef] [PubMed]
47. Eid, A.; Issa, L.; Al-kharouf, O.; Jaber, R.; Hreash, F. Development of *Coriandrum sativum* Oil Nanoemulgel and Evaluation of Its Antimicrobial and Anticancer Activity. *BioMed Res. Int.* **2021**, *2021*, 5247816. [CrossRef] [PubMed]

48. Chookiat, S.; Theansungnoen, T.; Kiattisin, K.; Intharuksa, A. Nanoemulsions Containing Mucuna pruriens (L.) DC. Seed Extract for Cosmetic Applications. *Cosmetics* **2024**, *11*, 29. [[CrossRef](#)]
49. Jusril, N.A.; Abu Bakar, S.I.; Khalil, K.A.; Md Saad, W.M.; Wen, N.K.; Adenan, M.I. Development and Optimization of Nanoemulsion from Ethanolic Extract of Centella asiatica (NanoSECA) Using D-Optimal Mixture Design to Improve Blood-Brain Barrier Permeability. *Evid.-Based Complement. Altern. Med.* **2022**, *2022*, 3483511. [[CrossRef](#)] [[PubMed](#)]
50. Ding, Z.; Jiang, Y.; Liu, X. Chapter 12—Nanoemulsions-Based Drug Delivery for Brain Tumors. In *Nanotechnology-Based Targeted Drug Delivery Systems for Brain Tumors*; Kesharwani, P., Gupta, U., Eds.; Academic Press: Cambridge, MA, USA, 2018; pp. 327–358.
51. Honary, S.; Zahir, F. Effect of Zeta Potential on the Properties of Nano-Drug Delivery Systems—A Review (Part 1). *Trop. J. Pharm. Res.* **2013**, *12*, 255–264. [[CrossRef](#)]
52. Sungpud, C.; Panpipat, W.; Chaijan, M.; Sae Yoon, A. Techno-biofunctionality of mangostin extract-loaded virgin coconut oil nanoemulsion and nanoemulgel. *PLoS ONE* **2020**, *15*, e0227979. [[CrossRef](#)] [[PubMed](#)]
53. Magalhães, D.; Vilas-Boas, A.A.; Teixeira, P.; Pintado, M. Functional Ingredients and Additives from Lemon by-Products and Their Applications in Food Preservation: A Review. *Foods* **2023**, *12*, 1095. [[CrossRef](#)]
54. Gadhave, D.; Tupe, S.; Tagalpallewar, A.; Gorain, B.; Choudhury, H.; Kokare, C. Nose-to-brain delivery of amisulpride-loaded lipid-based poloxamer-gellan gum nanoemulgel: In vitro and in vivo pharmacological studies. *Int. J. Pharm.* **2021**, *607*, 121050. [[CrossRef](#)] [[PubMed](#)]
55. Soliman, W.E.; Shehata, T.M.; Mohamed, M.E.; Younis, N.S.; Elsewedy, H.S. Enhancement of Curcumin Anti-Inflammatory Effect via Formulation into Myrrh Oil-Based Nanoemulgel. *Polymers* **2021**, *13*, 577. [[CrossRef](#)]
56. Sultan, M.H.; Javed, S.; Madkhali, O.A.; Alam, M.I.; Almoshari, Y.; Bakkari, M.A.; Sivadasan, D.; Salawi, A.; Jabeen, A.; Ahsan, W. Development and Optimization of Methylcellulose-Based Nanoemulgel Loaded with Nigella sativa Oil for Oral Health Management: Quadratic Model Approach. *Molecules* **2022**, *27*, 1796. [[CrossRef](#)] [[PubMed](#)]
57. Eid, A.M.; El-Enshasy, H.A.; Aziz, R.; Elmarzugi, N.A. Preparation, characterization and anti-inflammatory activity of Swietenia macrophylla nanoemulgel. *J. Nanomed. Nanotechnol.* **2014**, *5*, 1–10. [[CrossRef](#)]
58. Xi, W.; Lu, J.; Qun, J.; Jiao, B. Characterization of phenolic profile and antioxidant capacity of different fruit part from lemon (*Citrus limon* Burm.) cultivars. *J. Food Sci. Technol.* **2017**, *54*, 1108–1118. [[CrossRef](#)] [[PubMed](#)]
59. Diab, K.A. In Vitro Studies on Phytochemical Content, Antioxidant, Anticancer, Immunomodulatory, and Antigenotoxic Activities of Lemon, Grapefruit, and Mandarin Citrus Peels. *Asian Pac. J. Cancer Prev.* **2016**, *17*, 3559–3567. [[PubMed](#)]
60. Imran, M.; Basharat, D.; Khalid, S.; Aslam, M.; Syed, F.; Jabeen, S.; Kamran, H.; Muhammad, Z.; Shahid, M.Z.; Tufail, T.; et al. Citrus Peel Polyphenols: Recent Updates and Perspectives. *Int. J. Biosci.* **2020**, *16*, 53–70.
61. Shehata, M.G.; Awad, T.S.; Asker, D.; El Sohaimy, S.A.; Abd El-Aziz, N.M.; Youssef, M.M. Antioxidant and antimicrobial activities and UPLC-ESI-MS/MS polyphenolic profile of sweet orange peel extracts. *Curr. Res. Food Sci.* **2021**, *4*, 326–335. [[CrossRef](#)] [[PubMed](#)]
62. Saaty, A.H. Grapefruit Seed Extracts' Antibacterial and Antiviral Activity: Anti-Severe Acute Respiratory Syndrome Coronavirus 2 Impact. *Arch. Pharm. Pract.* **2022**, *13*, 69. [[CrossRef](#)]
63. Mejri, H.; Aidi Wannes, W.; Mahjoub, F.H.; Hammami, M.; Dussault, C.; Legault, J.; Saidani-Tounsi, M. Potential bio-functional properties of *Citrus aurantium* L. leaf: Chemical composition, antiviral activity on herpes simplex virus type-1, antiproliferative effects on human lung and colon cancer cells and oxidative protection. *Int. J. Environ. Health Res.* **2024**, *34*, 1113–1123. [[CrossRef](#)]
64. Tang, K.; He, S.; Zhang, X.; Guo, J.; Chen, Q.; Yan, F.; Banadyga, L.; Zhu, W.; Qiu, X.; Guo, Y. Tangeretin, an extract from Citrus peels, blocks cellular entry of arenaviruses that cause viral hemorrhagic fever. *Antivir. Res.* **2018**, *160*, 87–93. [[CrossRef](#)]
65. Meydanju, N.; Pirsa, S.; Farzi, J. Biodegradable film based on lemon peel powder containing xanthan gum and TiO<sub>2</sub>-Ag nanoparticles: Investigation of physicochemical and antibacterial properties. *Polym. Test.* **2022**, *106*, 107445. [[CrossRef](#)]
66. Miyake, Y.; Hiramitsu, M. Isolation and extraction of antimicrobial substances against oral bacteria from lemon peel. *J. Food Sci. Technol.* **2011**, *48*, 635–639. [[CrossRef](#)] [[PubMed](#)]
67. Albak, F.; TekİN, A.R. Development of Functional Chocolate with Spices and Lemon Peel Powder by using Response Surface Method: Development of Functional Chocolate. *Akad. Gida* **2014**, *12*, 19–25.
68. Çilingir, S.; Goksu, A.; Sabancı, S. Production of Pectin from Lemon Peel Powder Using Ohmic Heating-Assisted Extraction Process. *Food Bioprocess Technol.* **2021**, *14*, 1349–1360. [[CrossRef](#)]
69. Šafranko, S.; Šubarić, D.; Jerković, I.; Jokić, S. Citrus By-Products as a Valuable Source of Biologically Active Compounds with Promising Pharmaceutical, Biological and Biomedical Potential. *Pharmaceuticals* **2023**, *16*, 1081. [[CrossRef](#)]
70. Yabalak, E.; Erdoğan Eliuz, E.A.; Nazlı, M.D. Evaluation of Citrus reticulata essential oil: Chemical composition and antibacterial effectiveness incorporated gelatin on *E. coli* and *S. aureus*. *Int. J. Environ. Health Res.* **2022**, *32*, 1261–1270. [[CrossRef](#)]
71. Abirami, S.; Edwin Raj, B.; Soundarya, T.; Kannan, M.; Sugapriya, D.; Al-Dayan, N.; Ahmed Mohammed, A. Exploring antifungal activities of acetone extract of selected Indian medicinal plants against human dermal fungal pathogens. *Saudi J. Biol. Sci.* **2021**, *28*, 2180–2187. [[CrossRef](#)]